Supporting Information

Nanochannel-Based Heterometallic {$Zn^{II}Ho^{III}$}-Organic Framework with Highly Catalytic Activity on Chemical Fixation of CO_2

Tao Zhang,[a,b] Hongtai Chen,[a] Hongxiao Lv,[a] Qiaoling Li,[a,*] and Xiutang Zhang[a,*]

*North University of China, Taiyuan 030051, People's Republic of China; *E-mail: qiaolingl@163.com, xiutangzhang@163.com.*
Taiyuan Institute of Technology, Taiyuan 030008, People's Republic of China.

Contents

X-ray crystallography.

Single-crystal diffractometry for **NUC-30** was conducted on a Bruker Smart Apex CCD diffractometer of Bruker D8 VENTURE PHOTON II by employing graphite-monochromated Mo-Kα radiation (λ = 0.071073 nm) at 296(2) K and then corrected for Lorentz and polarization effects along with the multi-scan absorption by an correction SADABS program. Therefore, crystal structure was offered by direct methods and refined by full-matrix least-squares with the SHELXL (Sheldrick, 2015) package. Hydrogen atoms except those on water molecules were generated geometrically with fixed isotropic thermal parameters, and included in the structure factor calculations. The solvent content of **NUC-30** was determined with the help of the thermogravimetric analysis (Figure S2). Crystallographic data and refinement parameter were listed in Table S1. Selected bond lengths and angles were concluded in Table S2. Further details on the crystal structure investigations may be obtained from the Cambridge Crystallographic Data Centre, with the depository number CCDC-2036304 for **NUC-30**.

Table S1. Crystallographic data and refinement parameters of NUC-30.

Complex	**NUC-30**
Formula	$C_{29}H_{11}HoNO_{13}Zn$
Mr	811.71
Crystal system	Trigonal
Space group	R-3m
a (Å)	47.916 (16)
b (Å)	47.916 (16)
c (Å)	13.299 (4)
α (°)	90
β (°)	90
γ (°)	120
V(Å^3)	26443.9(2)
Z	18
Dcalcd(g·cm^{-3})	0.917
μ(mm^{-1})	3.249
GOF	1.028
R_1 [I＞2σ(I)]a	0.0460
wR_2 [I＞2σ(I)]b	0.1573
R_1[a](all data)	0.0479
wR_2[b] (all data)	0.1592
R_{int}	0.0289

[a] $R_1 = \sum||F_o|-|F_c|| / \sum|F_o|$. [b] $wR_2 = [\sum w(|F_o|^2-|F_c|^2)] / \sum|w(F_o^2)^2|^{1/2}$

Table S2. Selected bond lengths and angles of NUC-30.

NUC-30					
Ho(1)-O(1)	2.243(2)	O(2)-C(1)	1.254(4)	C(15)-C(19)	1.508(5)
Ho(1)-O(1)#1	2.243(2)	O(1)-C(1)	1.249(4)	C(15)-C(14)	1.305(6)
Ho(1)-O(7)#3	2.286(3)	O(7)-C(19)	1.224(5)	C(15)-C(16)	1.334(6)
Ho(1)-O(4)#2	2.369(3)	O(4)-C(8)	1.239(4)	C(11)-C(12)	1.481(5)
Ho(1)-O(4)#7	2.369(3)	N(1)-C(9)	1.372(4)	C(3)-C(2)	1.393(4)
Ho(1)-O(3)#2	2.436(3)	N(1)-C(9)#4	1.372(4)	C(2)-C(7)	1.394(4)
Ho(1)-O(3) #7	2.436(3)	O(3)-C(8)	1.237(4)	C(12)-C(13)	1.338(6)
Ho(1)-OW	2.346(4)	O(8)-C(19)	1.251(5)	C(12)-C(17)	1.331(7)
Ho(1)-C(8)#2	2.762(3)	C(9)-C(10)	1.368(4)	C(6)-C(7)	1.374(6)
Ho(1)-C(8)#7	2.762(3)	C(9)-C(5)	1.476(5)	C(14)-C(13)	1.376(7)
Zn(1)-O(5)#5	1.933(3)	C(10)-C(11)	1.363(4)	C(13)-C(18)	1.658(7)
Zn(1)-O(2)	1.964(3)	C(4)-C(5)	1.407(4)	C(13)-C(18)#4	1.658(7)
Zn(1)-O(2)#1	1.963(3)	C(4)-C(3)	1.381(5)	C(16)-C(17)	1.368(8)
Zn(1)-O(8) #3	1.918(3)	C(1)-C(2)	1.486(5)	C(18)-C(18)#4	1.593(17)
O(5)-C(18)	1.239(7)	C(5)-C(6)	1.387(5)	C(18)-O(6)	1.198(9)
O(5)-C(18)#2	1.239(7)				
Symmetry transformations used to generate equivalent atoms: #1 -x+y, +y, +z #2 -1/3+y, 1/3+x, 1/3-z; #3 1/3-x+y, 5/3-x, -1/3+z; #4 +x, 1+x-y, z; #5 -1/3+y, 1/3+x, 4/3-z; #6 4/3-x, 2/3-x+y, 2/3-z; #7 2/3+x-y, 1/3+x, 1/3-z.					

Table S3. The molecular size of various substituted epoxides.

Entry	Epoxides	Molecular size[a] (Å)
1	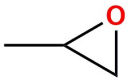	6.145*4.454*5.035
2	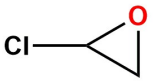	6.121*4.397*5.046
3	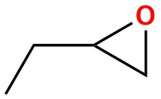	7.144*5.296*5.084
4	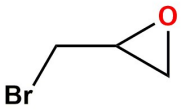	7.202*5.611*5.089
5	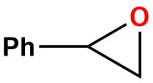	9.323*6.898*4.646
6	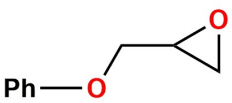	11.208*6.765*4.823

[a] van der Waals radii were determined by Bondi.

Table S4. Comparison of the catalytic performance of NUC-30 catalyst with selected previously reported MOFs.

MOF	Catalyst (mol %)	Temperature	Pressure (MPa)	Time	Yield (%)	Ref.
MOF-205(M)	2.5	RT	0.4	4	80	S1
NH2-MIL-101(Al)	0.17	120	1.8	6	95	S2
MMCF-2	0.13	RT	0.1	48	95	S3
Cr-MIL-101	1.2	RT	0.8	24	82	S4
UiO-67	1.5	90	0.1	12	95	S5
MOF-893	0.32	80	0.1	23	88	S6
M-MOF-184	1.2	80	0.1	6	82	S7
NUC-30	1.0	60	1.0	8	98	This work

Table S5. The ICP measurement results.

Fluorescence experiment of **NUC-30**	Initial	After sensing measurement
The concentration of Fe^{3+} ($mol \cdot L^{-1}$)	1.0×10^{-2}	9.97×10^{-3}

ICP measurements:

After the fluorescence experiment, the suspension was filtered. And filter cake (**NUC-30**) was washed several times with fresh solvent. Then, ICP measurements were performed on the filtrate (solution containing Fe^{3+} ions), the results were listed in Table S5.

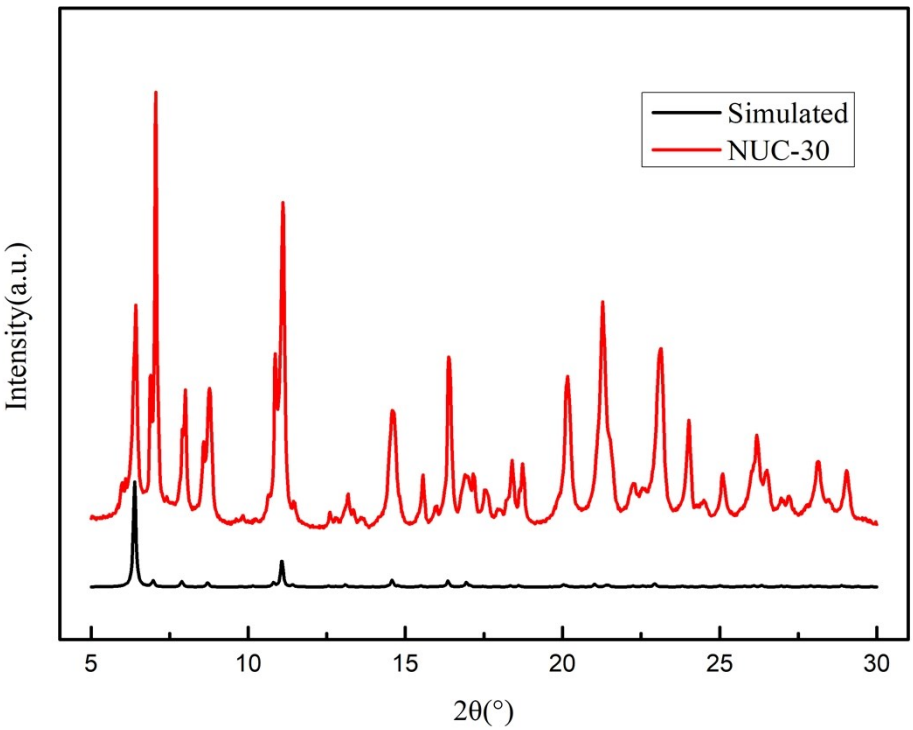

Figure S1. PXRD pattern of NUC-30 and simulated

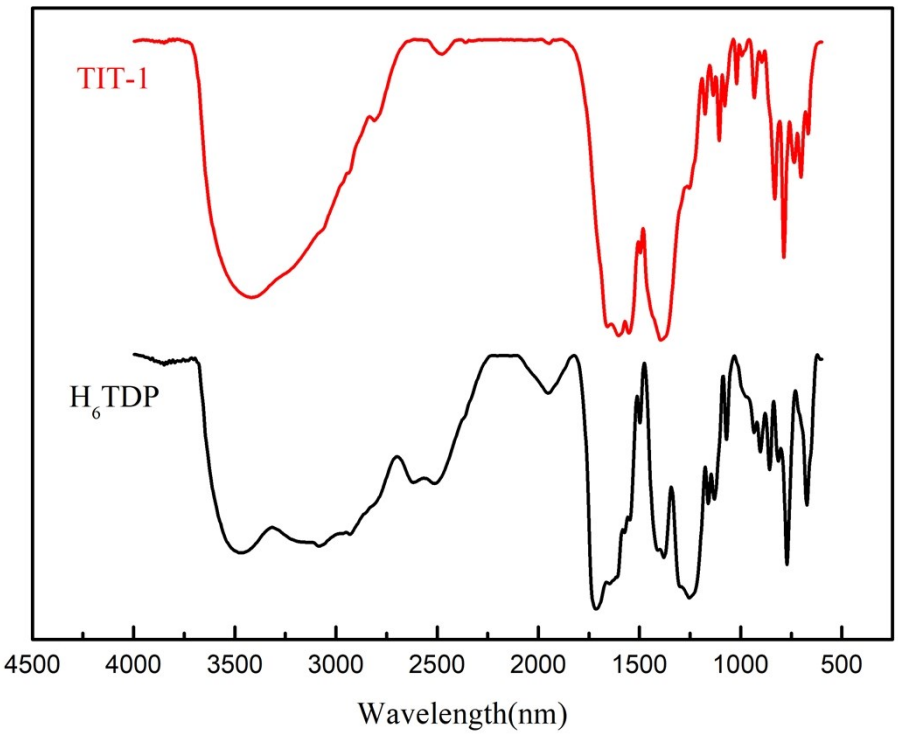

Figure S2. IR spectrum of as-synthesized NUC-30.

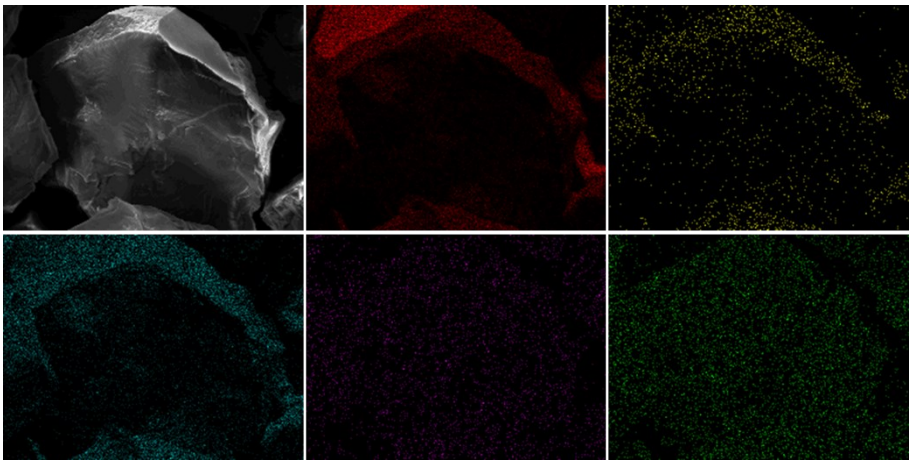

Figure S3. SEM-EDS images of NUC-30 (C: Red；N: Yellow; O: Cyan; Zn: Purple; Ho: Green)

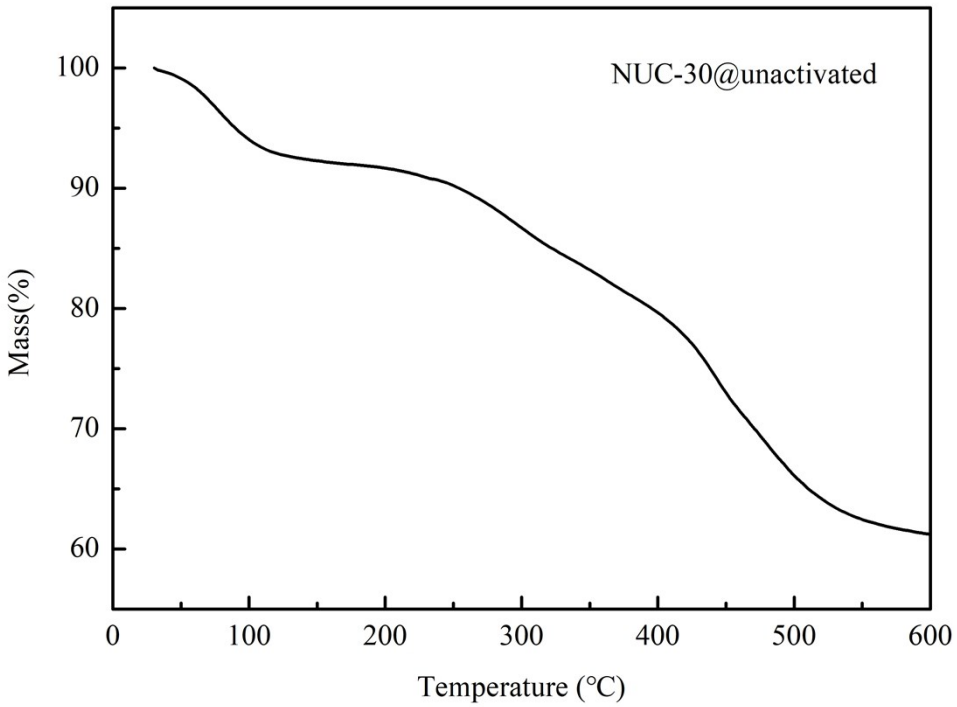

Figure S4. TGA curve of as-synthesized sample of NUC-30.

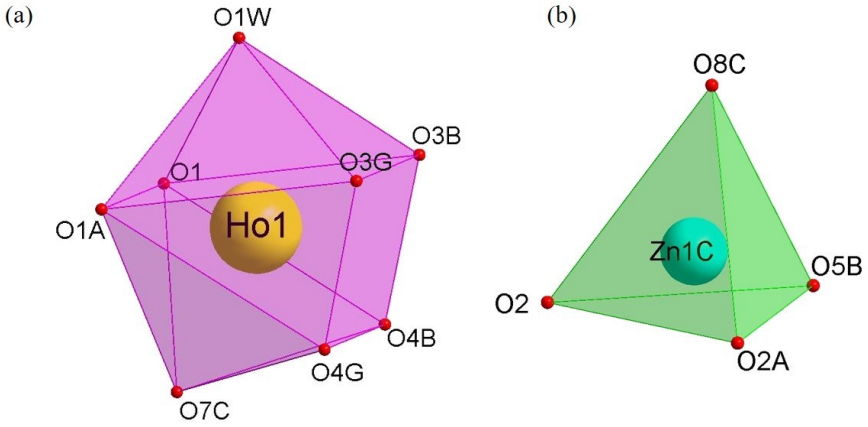

Figure S5. Ho-o polyhedral structure(a), Zn-o tetrahedral structure(b).

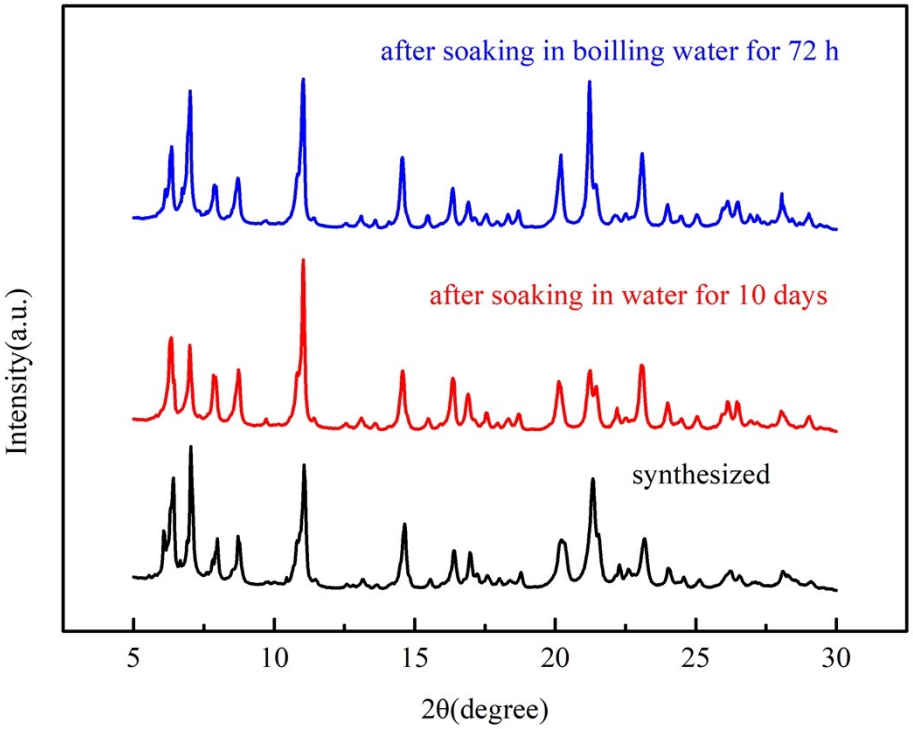

Figure S6. PXRD patterns of NUC-30 under water treatment.

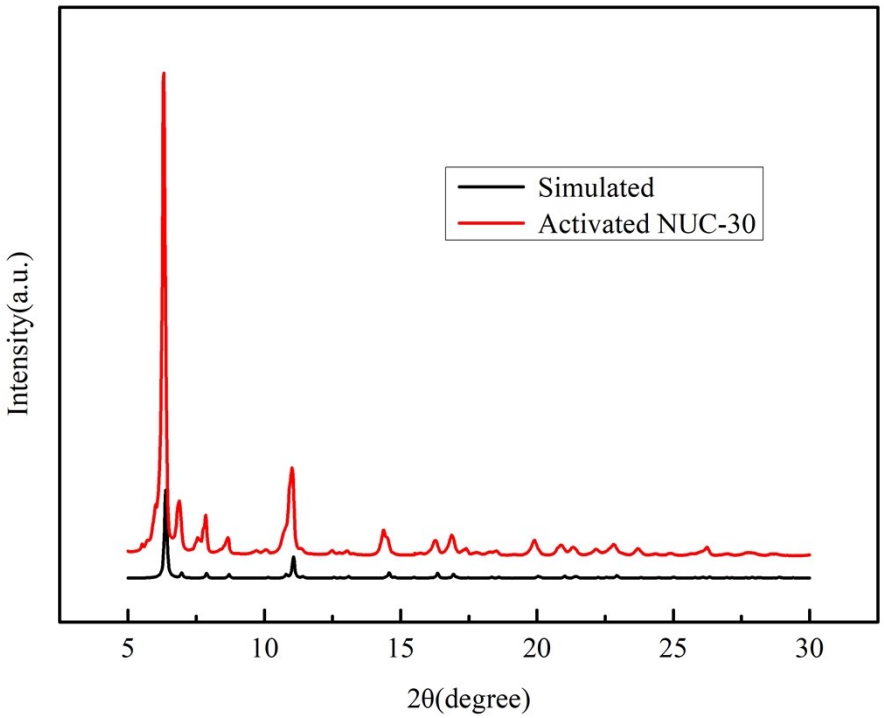

Figure S7. PXRD pattern of activated NUC-30 and simulated

Isosteric Heat Calculation.

The Q_{st} value is a parameter describing the average adsorption enthalpy of adsorbed gas molecules within a specific surface coverage. It is usually evaluated by two or more adsorption isotherms collected at similar temperatures. The method of calculating the isothermal heat of zero cover adsorption is to first synthesize the temperature related isotherm data into a dimensional expression, which can be written as:

$$lnP = lnN + \frac{1}{T}\sum_{i=0}^{m} a_i N^i + \sum_{i=0}^{n} b_i N^i$$

$$Q_{st} = -R\sum_{i=0}^{m} a_i N^i$$

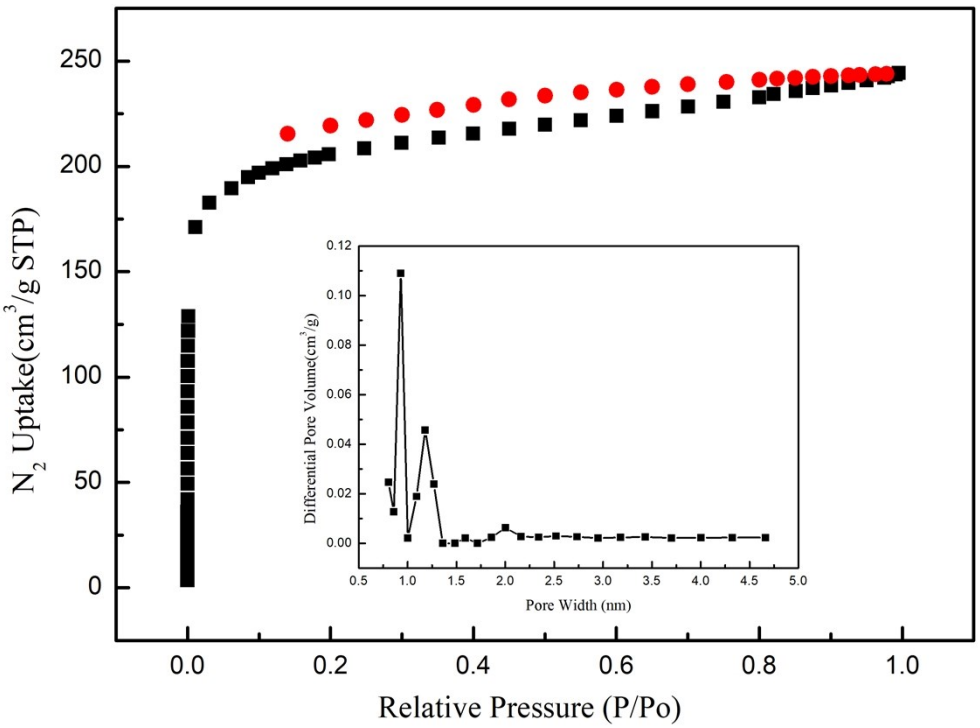

Figure S8. N_2 absorption and desorption isotherms of NUC-30 at 77 K (Insert: the pore size distribution)

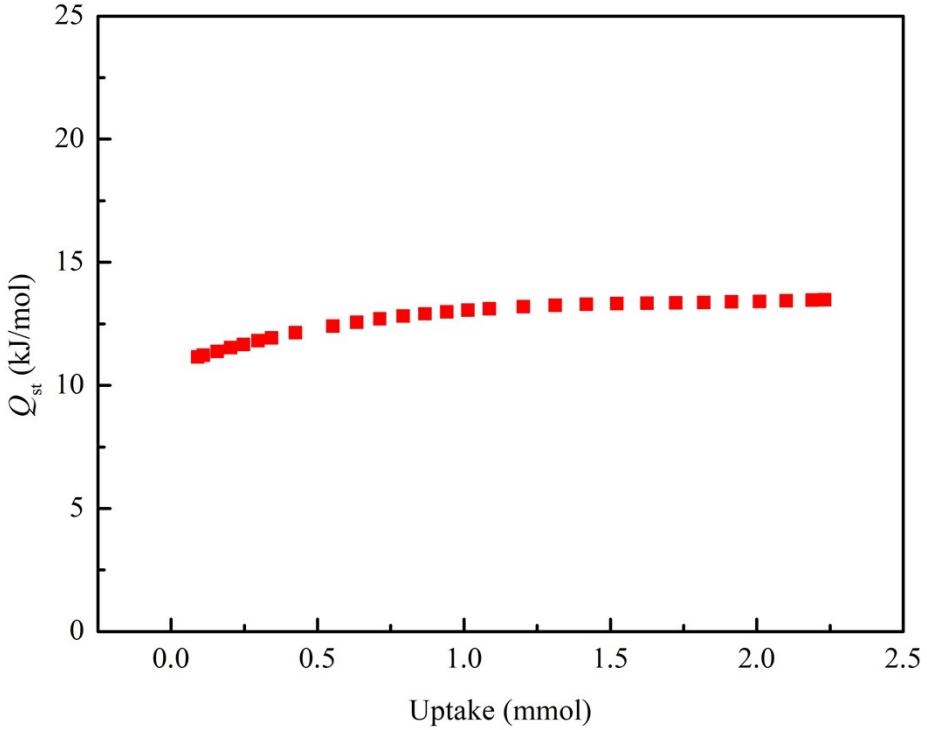

Figure S9. CO_2 adsorption heat calculated by the virial equation of NUC-30.

5

Yield Calculation Based on the GC-MS Analysis

Gas chromatography mass spectrometry (GC-MS) analyses were executed on a time-of-flight Thermo Fisher Trace ISQ GC/MS instrument, the yield (%) was calculated based on the consumption of starting material using the equation:

$$Yield\ (\%) = \left(\frac{\frac{area\ of\ reactant\ at\ 0\ hour}{area\ of\ interal\ standard\ at\ 0\ hour} - \frac{area\ of\ reactant\ at\ any\ time}{area\ of\ interal\ standard\ at\ any\ time}}{\frac{area\ of\ reactant\ at\ 0\ hour}{area\ of\ interal\ standard\ at\ 0\ hour}} \right) \times 100\%$$

5

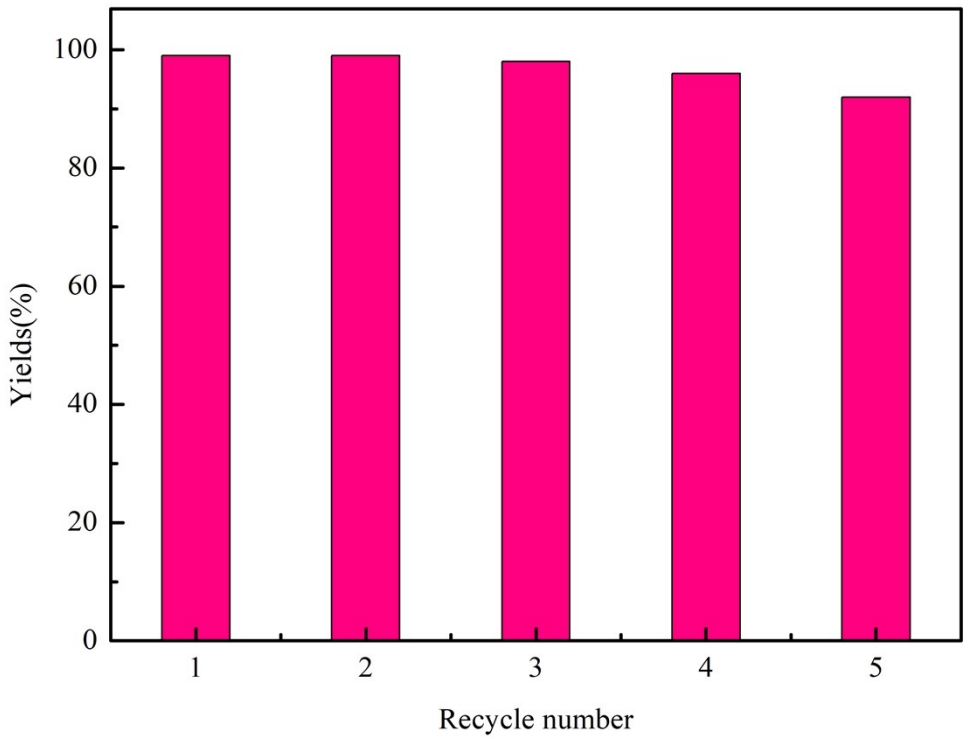

Figure S10. The recycled cycloaddition reaction of CO_2 with styrene oxide.

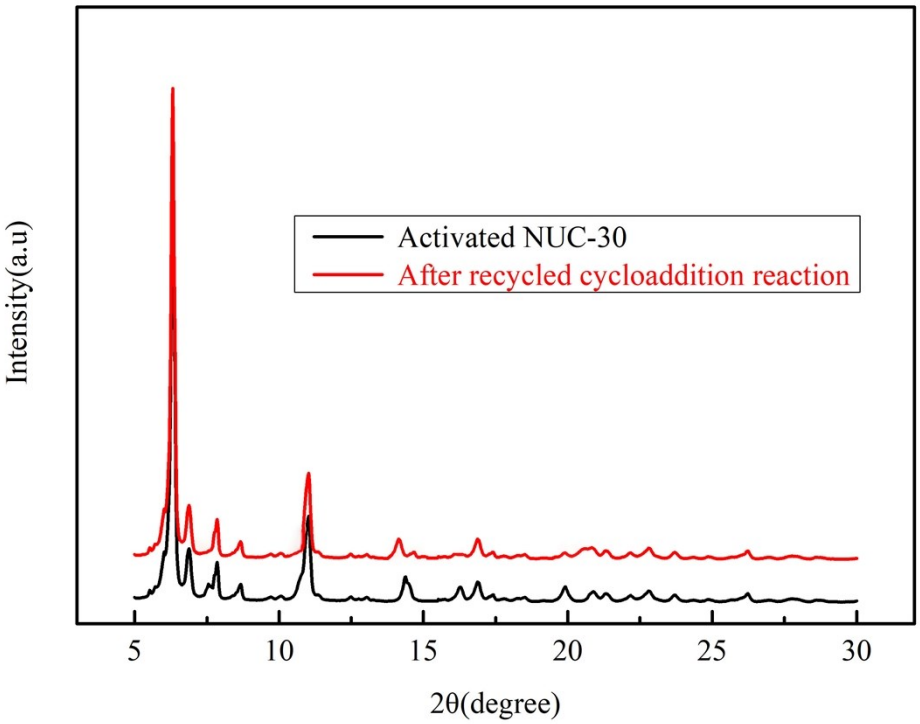

Figure S11. The PXRD pattern of NUC-30 after recycled cycloaddition reaction.

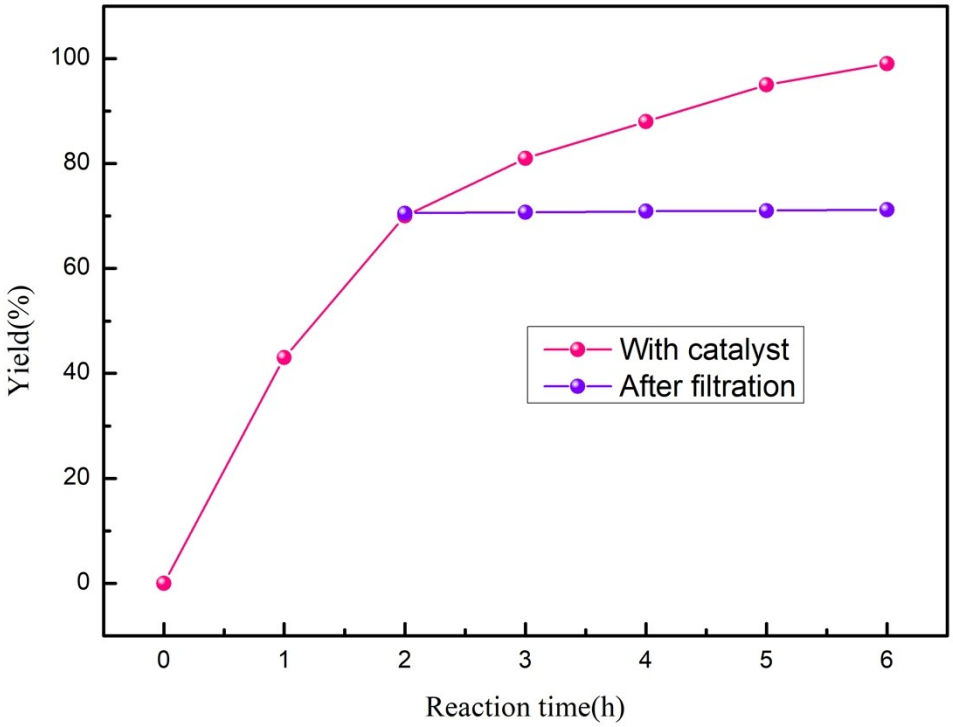

Figure S12. Evidence of heterogeneous nature of NUC-30 in the coupling of chloromethyloxiran with CO_2.

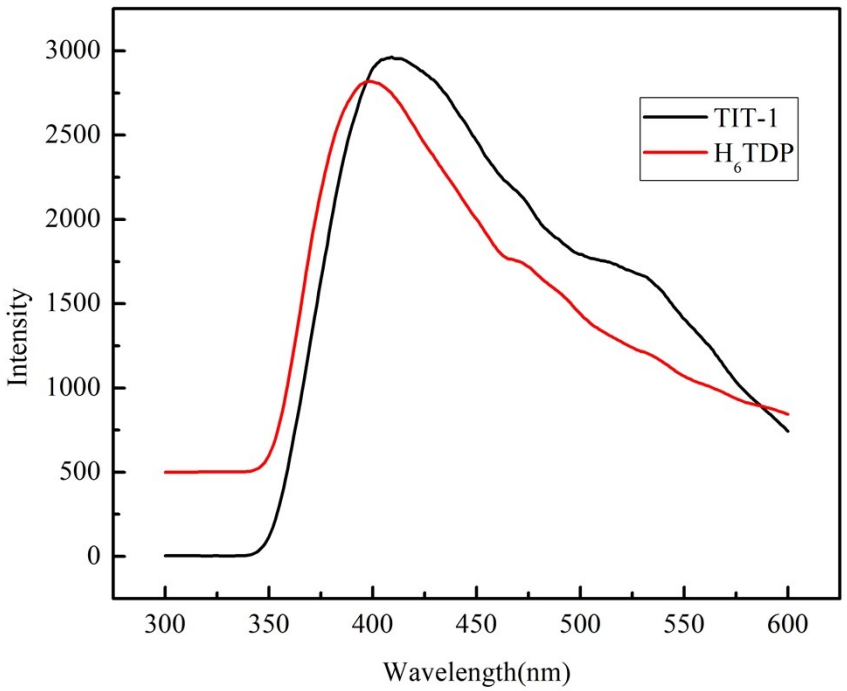

Figure S13. The fluorescent emission curves of NUC-30(black) and ligand H_6TDP (red).

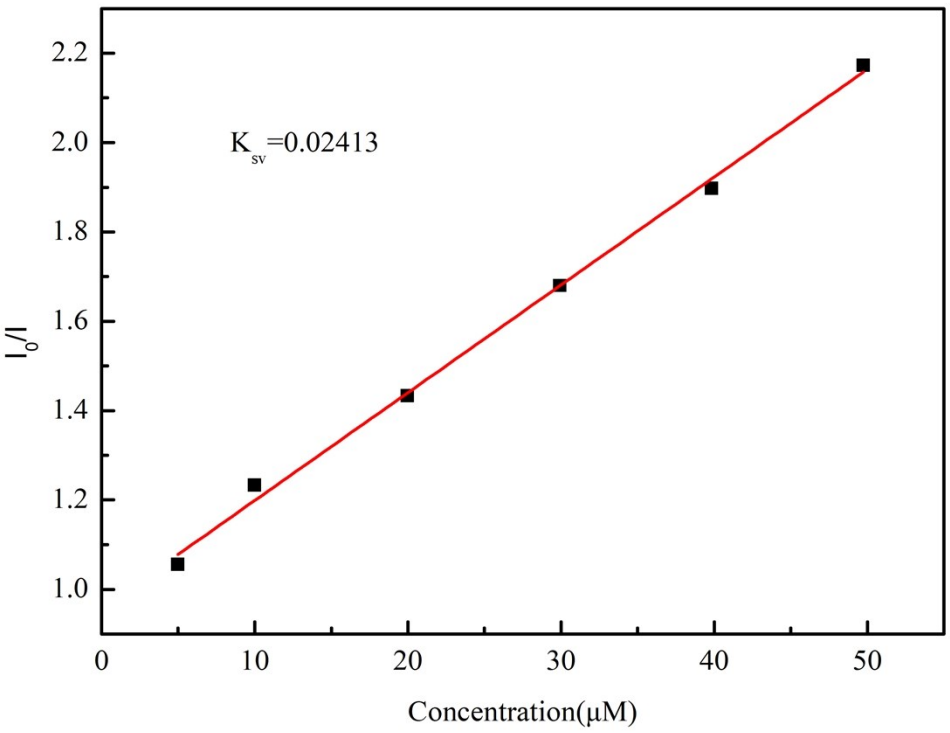

Figure S14.The fitting experimental data with low concentration range of Fe^{3+}.

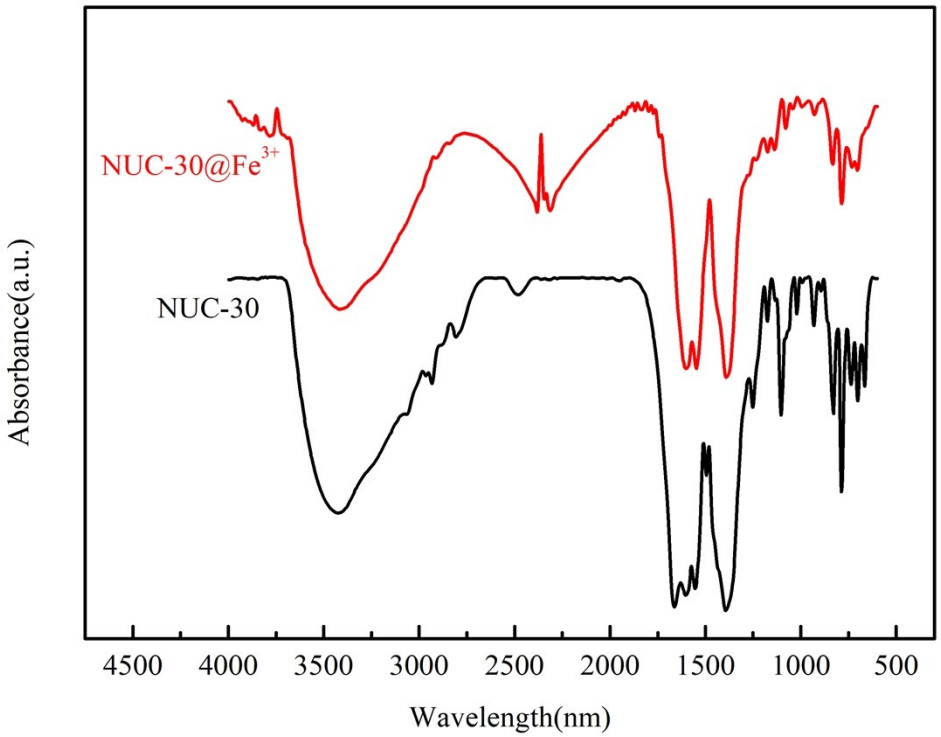

Figure S15. IR spectrum of NUC-30 under fluorescence quenching of different ions.

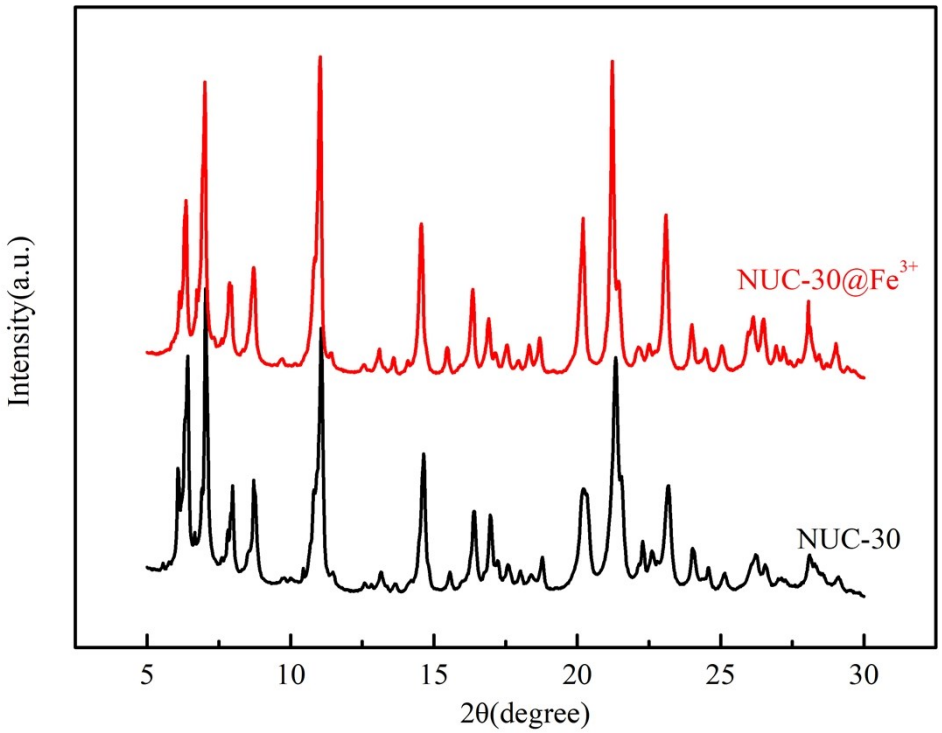

Figure S16. PXRD patterns of NUC-30 under fluorescence quenching of different ions.

Reference

S1. Babu, R. Roshan, R.; Kathalikkattil, A. C.; Kim, D. W.; Park D.-W. Rapid. *ACS Appl. Mater. Interfaces* **2016**, *8*, 33723−33731.

S2. Senthilkumar, S.; Maru, M. S.; Somani, R. S.; Bajaj, H. C.; Neogi, S. *Dalton Trans*. **2018**, *47*, 418−428.

S3. Gao, W. Y.; Chen, Y.; Niu, Y. H.; Williams, K.; Cash, L.; Perez, P. J.; Wojtas, L.; Cai, J. F.; Ma, S. Q. *Angew. Chem., Int. Ed*. **2014**, *53*, 2615−2619.

S4. Zalomaeva, O. V.; Chibiryaev, A. M.; Kovalenko, K. A.; Kholdeeva, O. A.; Balzhinimaev, B. S.; Fedin, V. P. *J. Catal*. **2013**, *298*, 179−185.

S5. Luo-Gang Ding, Bing-Jian Yao, Wei-Ling Jiang, Jiang-Tao Li, Qi-Juan Fu, Yan-An Li, Zhen-Hua Liu, Jian-Ping Ma, Yu-Bin Dong. *Inorg. Chem.* **2017**, *56*, 2337−2344.

S6. Phuong T. K. Nguyen, Huong T. D. Nguyen, Hung N. Nguyen, Christopher A. Trickett, Quang T. Ton, Enrique Gutié rrez-Puebla, M. Angeles Monge, Kyle E. Cordova, Felipe Gá ndara. *ACS Appl. Mater. Interfaces.* **2018**, *10*, 733−744.

S7. Y. B. N. Tran, Phuong T. K. Nguyen, Quang T. Luong, Khoi D. Nguyen. *Inorg. Chem*. **2020**, *59*, 16747−16759.